CMS Physics Analysis Summary

Contact: cms-pag-conveners-exotica@cern.ch 2016/11/08

Search for low-mass pair-produced dijet resonances using jet substructure techniques in proton-proton collisions at $\sqrt{s} = 13$ TeV

The CMS Collaboration

Abstract

Results from a search for paired boosted diquark resonances, using jet substructure techniques, are reported. This search uses data corresponding to an integrated luminosity of 2.7 fb^{-1} from proton-proton collisions at a center-of-mass energy of $\sqrt{s} = 13$ TeV, recorded by the CMS detector at the LHC in 2015. Limits at 95% confidence level are set on the production of top squarks decaying to two light quarks in the framework of R-parity violating supersymmetry. Top squarks with masses between 80 and 240 GeV are excluded.

1 Introduction

Many beyond the standard model (BSM) scenarios in particle physics incorporate particles that decay into fully hadronic final states. Supersymmetric (SUSY) models are standard model (SM) extensions, which simultaneously solve the hierarchy problem and unify particle interactions [1, 2]. In natural SUSY models, where there is minimal fine-tuning, the top quark superpartner (top squark or stop) and the superpartners of the Higgs boson (higgsinos) are required to be light [3–7]. Natural SUSY is under-constrained in certain R-parity violating (RPV) scenarios [8]. R-parity is a quantum number defined as $R = (-1)^{3B+L+2S}$, where B and L are the baryon and lepton numbers, respectively, and S is the spin. The RPV superpotential, W, is defined as

$$W = \frac{1}{2}\lambda_{ijk}L_iL_jE^c_k + \lambda'_{ijk}L_iQ_jD^c_k + \frac{1}{2}\lambda''_{ijk}U^c_iD^c_jD^c_k + \mu'_iL_iH_u \tag{1}$$

where λ_{ijk}, λ'_{ijk}, λ''_{ijk} and μ'_i are trilinear couplings of each term, L_i are the left-handed lepton doublets, E_i are the right-handed lepton doublets, Q_i the left-handed quark doublets, U_i and D_j are right-handed quarks, H_u is the Higgs that gives mass to the up-type quarks and $i, j, k = 1, 2, 3$ are generation indices while the superindex c is the charge conjugation.

Such a superpotential contains terms which violate lepton number (1st and 2nd term in equation (1)) or baryon number (3rd term), leading to a rapid decay of protons [9]. Assuming R-parity conservation, the coupling constants of these terms vanish or they are sufficiently small for the lifetime of the proton to be compatible with the SM. Under RPV, the coupling of the hadronic term of the potential (λ''_{ijk}) or the leptonic term (λ_{ijk}) or the mixture of the two (λ'_{ijk}) may be non-zero. For instance, a non-zero hadronic RPV term would produce decays of squarks into multiple quarks in the final state with no missing energy or leptons, while a non-zero leptonic RPV term could yield sleptons decaying into a pair of leptons.

We present the results of a search for pair production of resonances decaying to pairs of light-flavor quarks in events where the resonant particles are boosted (i.e. produced with large transverse momentum such that the decay products are close together) resulting in a final state with two massive jets. We use the pair production of stops decaying to light quarks via hadronic RPV (Figure 1) as the benchmark model of this analysis. A previous search by CDF [10] at the Fermilab Tevatron placed limits on the production cross sections possible in such models, excluding stop masses between 50 and 100 GeV. In Run I of the LHC, CMS excluded this model for stop masses between 200 and 350 GeV [11]. In Run II, ATLAS extended this exclusion for stop masses from 250 GeV to 405 GeV and between 445 and 510 GeV [12]. For the related light-quark plus b-quark decay channel, the CMS stop mass exclusion is between 200 and 385 GeV [11], while for ATLAS [13] it is between 100 and 310 GeV at 8 TeV (the only one exploiting the boosted regime), and from 250 to 345 GeV at 13 TeV [14].

The analysis presented here is based on data corresponding to 2.7 fb^{-1} [15] of integrated luminosity from proton-proton collisions at $\sqrt{s} = 13$ TeV, collected with the CMS detector [16] at the CERN LHC in 2015. At this collision energy, particles with low mass can be produced with significant momentum and their decay products will be Lorentz boosted, resulting in collimated fragmentation products. We are therefore able to reconstruct the particle's decay products as a single jet with a large cone size. These jets will differ from QCD jets in their internal structure and this analysis exploits this feature to reduce QCD and other SM backgrounds. Such boosted topologies have been explored using several grooming and substructure techniques developed in recent years [17, 18], and CMS has studied them in great detail [19]. Grooming techniques

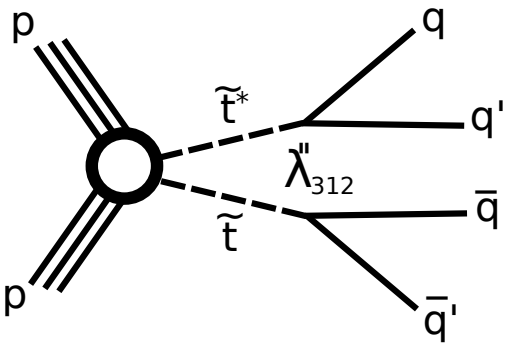

Figure 1: Direct pair production of stops decaying via the hadronic RPV coupling λ''_{312} into two light quarks.

remove extra components inside jets to bring their mass closer to the value of the initial parton. Substructure variables distinguish between jets coming from massive particle decays and those coming from the hadronization of single quarks or gluons [17].

In this analysis, we select events with at least two jets and high hadronic activity quantified as the scalar sum of the transverse momentum (p_T) of all jets with respect to the beam direction. The average jet mass distribution of the two leading jets, which is representative of pair-produced diquark resonances such as the stop, is investigated for evidence of a signal consistent with localized deviations from the estimated SM backgrounds. The main non-resonant background coming from QCD multijets is estimated using a technique relying on data, whereas the leading resonant backgrounds are estimated using Monte Carlo (MC) samples. SM MC samples are also used to optimize the signal selection and to evaluate systematic uncertainties.

2 CMS experiment

The central feature of the CMS apparatus [16] is a superconducting solenoid providing a magnetic field of 3.8 T. Within the superconducting solenoid volume are silicon pixel and strip trackers, a lead tungstate electromagnetic calorimeter (ECAL), and a hadron calorimeter (HCAL), which is made of interleaved layers of scintillator and brass absorber. Muons are measured in gas ionization detectors embedded in the steel return yoke outside the solenoid. A more detailed description of the CMS detector, together with a definition of the coordinate system used and the relevant kinematic variables, can be found in Ref. [16].

3 Event Simulation

The pair production of stops is simulated using the MADGRAPH 5_aMC@NLO v5.2.2.2 [20] event generator at leading order, and their decays are simulated using the PYTHIA v8.205 [21] MC program. Stop signal events are generated with up to two additional initial-state partons, and each stop decays into two quarks through the λ''_{UDD} quark RPV coupling. This coupling λ''_{312}, where the three numerical subscripts refer to the generations of the corresponding quarks, is set to a non-zero value such that the decay of the stop to two light-flavor jets is allowed. The

branching fraction of the stop decaying into two quarks is set to 100%. For the generation of this signal, all superpartners, except the stops, are taken to be decoupled [22–26] and no intermediate particles are produced in the stop decay. Stops are generated with masses from 80 GeV to 250 GeV in 10 GeV steps, with an additional sample at a mass of 300 GeV. The cross section calculations [27] are made at next-to-leading order (NLO) with next-to-leading-logarithm (NLL) corrections [28–33]. The natural width of the signal resonance is taken to be much smaller than the resolution of the detector.

Backgrounds from SM QCD multijet processes are simulated and showered through PYTHIA using the CUETP8M1 tune [34]. We also study additional SM backgrounds: the W+jets, Z +jets, ZZ and WW samples are generated with MADGRAPH 5_aMC@NLO, WZ processes are generated with PYTHIA, and the $\mathrm{t\bar{t}}$ sample is generated with POWHEG v2 [35–37]. The simulation of the CMS detector for all samples is performed with GEANT4 [38].

4 Trigger and Event Reconstruction

The data used in this analysis was recorded by the CMS detector over the entire 2015 LHC data-taking period with a multilevel trigger system. Physics objects in CMS are reconstructed using the particle flow (PF) algorithm [39] which uses information from every subdetector to build particle candidates like muons, photons, electrons and hadrons. The four-momenta of the particle candidates, after removing pileup contributions, are used to reconstruct jets with the jet clustering algorithm anti-k_{T} [40] with a distance parameter R in $\eta - \phi$ space using the FASTJET package [41].

Events are selected online using the logical OR of two sets of triggers based on the total hadronic transverse energy in the event (H_{T}). One trigger uses anti-k_{T} jets with $R = 0.8$ (AK8), an H_{T} threshold of 650 GeV using jets with $p_{\mathrm{T}} > 150$ GeV and $|\eta| < 2.5$, and the presence of at least one jet with a mass above 50 GeV using the *trimming* algorithm [42] (further described below) for jet grooming. The other trigger considers anti-k_{T} jets with $R = 0.4$ (AK4), jet $p_{\mathrm{T}} > 40$ GeV and $|\eta| < 3.0$, and $H_{\mathrm{T}} > 800$ GeV. The trigger selection is fully efficient for events with offline H_{T} above 900 GeV using AK8 jets with $p_{\mathrm{T}} > 150$ GeV and $|\eta| < 2.5$.

Jet energy scale corrections [43] are applied to jets to account for the combined response function of the detector to hadrons. The corrections are derived from MC simulation and are confirmed with in-situ measurements of the energy balance of dijet and photon+jet events. In data, a small residual correction factor is included to account for differences in jet response between data and simulation. To remove misidentified jets, which arise primarily from calorimeter noise, jet quality criteria [44] are applied. The efficiency of these criteria for signal events is above 99%.

Jet grooming techniques are used in order to improve the jet mass resolution and to reduce the pileup contributions in the jet mass. The main goal of these methods is to recluster the constituents of the jet while using additional information and requirements to eliminate soft, large-angle QCD radiation. In this analysis, we use the *trimming* algorithm [42] for the trigger and the *pruning* algorithm [45] for the analysis.

Within the constituents of the jet, *trimming* discriminates particles based on a dynamic p_{T} threshold. The algorithm reclusters the constituents of the original jet with a smaller cone size using the k_{T} algorithm [40]. Trimming accepts only the resulting subjets with a certain fraction of the p_{T} of the original jet. We use the *trimming* algorithm with subjets of $R = 0.1$ and containing at least 30% of the p_{T} of the original jet.

In the case of *pruning*, the constituents of the original jet are reclustered with the same cone size but using a modified Cambridge-Aachen (CA) algorithm [40]. Constituents i and j are merged in the reclustering algorithm if they satisfy at least one of the following conditions: $\min(p_{\mathrm{T}}^i, p_{\mathrm{T}}^j)/p_{\mathrm{T}}^{i+j} > z_{cut}$ and $\Delta R_{ij} < 2 \times r_{cut} \times m_J/p_{\mathrm{T}}$, where $\Delta R = \sqrt{(\Delta\eta)^2 + (\Delta\phi)^2}$, $\Delta\eta$ and $\Delta\phi$ are the differences in η and ϕ between the constituents, z_{cut} and r_{cut} are parameters of the algorithm, while m_J and p_{T} are the mass and the transverse momentum of the originally-clustered jet. If both conditions are not met, the softer of the two constituents is removed. We use $z_{cut} = 0.1$ and $r_{cut} = 0.5$.

To increase the discrimination between SM-like jets and the stop signal, we further select events based on so-called *N-subjetiness* [46]. This method exploits the difference in the expected energy flow between the radiation pattern from boosted hadronic resonances and jets coming from hadronization of single quarks or gluons, by counting the number of hard lobes of energy inside a jet. N-subjetiness uses the k_{T}-algorithm to recluster the constituents of the jet until N subjets are found. These N subjets are used to calculate the quantity:

$$\tau_N = \frac{1}{d_0} \sum_k p_{\mathrm{T},k} \times \min(\Delta R_{1,k}, \Delta R_{1,k}, ...\Delta R_{N,k}) \tag{2}$$

where $p_{\mathrm{T},k}$ is the transverse momentum of the k-th jet constituent and $\Delta R_{N,k}$ is the distance to the N-th subjet axis, the parameter $d_0 = \sum_k p_{\mathrm{T},k} \times R_0$ is a normalization factor, where R_0 is the cone size of the original jet. In this analysis we do not use the N-subjetiness variables by themselves but the ratio $\tau_{21} = \tau_2/\tau_1$, as this provides better discrimination between signal and background.

5 Event Selection

Events passing the trigger requirements are selected if they contain at least two jets with a minimum p_{T} of 150 GeV and $|\eta| < 2.5$. The transverse momentum of those jets are added together to evaluate H_{T}, and we select events with $HT > 900$ GeV, to ensure we are in a kinematic regime where the trigger is fully efficient.

The *pruning* algorithm is used to compute the masses of the two leading jets, ordered in p_{T}. The average mass of these two pruned jets, defined as $(m_{j1} + m_{j2})/2$, is used to investigate the presence of pair produced boosted resonances. In order to reduce the events coming from known SM processes, we apply selection criteria on the *mass asymmetry* variable defined as $M_{asym} = |m_{j1} - m_{j2}|/(m_{j1} + m_{j2})$, on the ratio of the N-subjetiness variables $\tau_{21} = \tau_2/\tau_1$ for both jets, and on the absolute value of the difference in η between the two jets used in the analysis, $|\eta_{j1} - \eta_{j2}|$. We optimize the selection criteria placed on these variables using the MC signal and backgrounds described in Section 3. Our strategy is to maximize the signal significance by using $S/\sqrt{B}$ as the metric, where S and B are the number of signal and background events, respectively, and B is determined by using the sum of the simulated SM events. The values of S and B are set to the number of events within a window of width 20 GeV centered at the generated stop mass. A common set of selection criteria was obtained and found to be close to optimal for every signal mass hypothesis considered. The final selection criteria are summarized in Table 1.

After all selection requirements are applied, the fraction of signal events remaining ranges from 0.005% at a stop mass of 80 GeV, increases to 0.1% for stop masses near 200 GeV, and drops to 0.001% for higher masses near 300 GeV, since the fraction of stops that are boosted decreases.

The low efficiencies in the selection of such boosted events are compensated by the large signal cross sections for low mass stop quarks; in addition, we find that this analysis has comparable sensitivity when comparing to previous searches mentioned in Section 1, for the same RPV scenario and in the region where the probed resonance masses are overlapping.

Table 1: Summary of variables used in the analysis and the corresponding optimized selection.

Variable	Selection
Number of AK8 jets	2 leading p_{T} jets
jet p_{T}	> 150 GeV
jet $\lvert\eta\rvert$	< 2.5
H_{T}	> 900 GeV
M_{asym}	< 0.1
$\lvert\eta_{j1} - \eta_{j2}\rvert$	< 1.5
1st and 2nd jet τ_{21}	< 0.45

6 Background Estimate

This analysis uses the spectrum of the average jet mass of the two leading pruned jets to search for resonances in the mass range 60-350 GeV. After applying the selection described in Table 1, we find that there are two types of important background components: the dominant non-resonant background composed mainly of QCD multijets, and resonant background components, composed primarily of $\mathrm{t\bar{t}}$ and W+jets, as well as Z +jets and diboson processes which are negligibly small. We model these two types of backgrounds in different ways. The non-resonant QCD multijets background is estimated primarily using data, while we rely on MC samples for the leading resonant backgrounds.

For the estimation of the non-resonant QCD multijets background we use a technique that relies on the data. In this method, which we refer to as "ABCD", we define regions in a 2-dimensional (2D) space based on two (uncorrelated) kinematic variables where one region is dominated by signal and the other three regions by background events. We use the M_{asym} and $|\eta_{j1} - \eta_{j2}|$ variables to define the 2D space since we found the correlation between these variables to be small. Then, we use these two variables to build the four regions identified in Table 2. Region A is defined by the nominal selection criteria for the signal region, B and C are sideband regions where the selection of only one of the two variables is applied, and region D is defined as the region when both selection criteria fail. Additionally, to ensure that this method models the non-resonant background only, and to avoid double counting of backgrounds, we subtract from the data in regions B, C, and D the expected resonant background contributions obtained from MC. The overall background estimate (both yield and shape) is then derived as a projection into the signal region (A) by calculating: $(B \times C)/D$. First, we evaluate the ratio B/D, which we consider as a "transfer factor" to be applied to events in region C. We parameterize the transfer factor by fitting the ratio B/D in data and then apply it to region C in each average mass bin. We find that this ratio as a function of average pruned jet mass is well modeled by a sigmoid function of the form: $1/(p_0 + \exp(p_1 + p_2 x^3))$; the fit of the ratio in the data and in the SM MC give consistent results. We test the robustness of this background method by using the transfer factor fit from the SM MC and apply it to region C in the SM MC; this ABCD prediction is then compared to the background prediction in the signal region (A) using SM MC only. The level of disagreement of the two background predictions, or closure, is found to be within $\pm 10\%$ over the whole mass spectrum and is used as a systematic uncertainty on the yield of the ABCD background prediction.

Table 2: Definition of the regions A, B, C, D for the ABCD method.

	$M_{asym} < 0.1$	$M_{asym} > 0.1$
$\lvert\eta_{j1} - \eta_{j2}\rvert > 1.5$	Region B	Region D
$\lvert\eta_{j1} - \eta_{j2}\rvert < 1.5$	Region A	Region C

For the resonant backgrounds we rely on the use of the MC, but tested in a data control region. A $t\bar{t}$ control region is selected by applying b-jet tagging to both AK8 jets, in addition to the nominal event selection. The algorithm used to tag b-quarks in this study is referred to as combined inclusive secondary vertex (CSVv2) [47], with the medium working point which has an efficiency of $\approx$ 69%. We find that the $t\bar{t}$ MC is underestimated in this control region by a factor of 1.5 ± 0.24. To correct this discrepancy in MC, we apply a scale factor of 1.5 to the $t\bar{t}$ MC, to which we conservatively assign a 50% systematic uncertainty. In the case of the remaining resonant backgrounds (W+jets, Z+jets and dibosons), we similarly assign a conservative 50% systematic uncertainty on the MC modeling.

Figure 2 shows the comparison of the data in the signal region with the final total background prediction. This background estimate is the sum of the ABCD method from data for the non-resonant QCD multijets background, and the sub-dominant resonant backgrounds from MC; $t\bar{t}$ and W+jets, correspond to less than 5% and 2% of the total background, respectively, whereas Z +jets and dibosons combined are $<$ 1% of the total background.

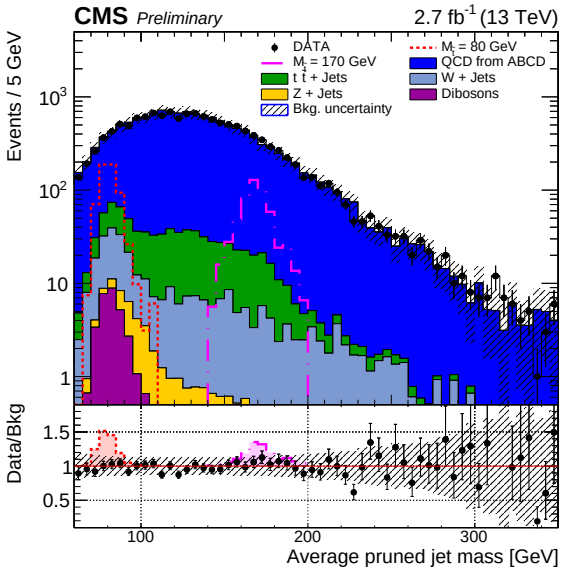

Figure 2: Average pruned jet mass distribution shown for data (dots) and the total background prediction. The different background components are shown with different colors while the grey hashed band shows the total background uncertainty. On the bottom, ratio between data and background prediction, with the grey hashed band showing the total background uncertainty. The background uncertainties are described in Section 7 and summarized in Table 4. The shaded colored regions on the bottom indicate the expected top squark signal distributions shown for two different selected masses as they would appear in data.

7 Systematic Uncertainties

We consider systematic uncertainties on the signal yield and on the background estimation.

The systematic uncertainties we consider that affect the signal acceptance are summarized in Table 3. Uncertainties on the reconstruction of jets affect the signal acceptance as well as the shape of the reconstructed resonance in the signal samples. The four-momenta of the reconstructed jets are rescaled (smeared) according to the uncertainties on the measured jet energy scale (jet energy resolution) [43]. The signal acceptances are reevaluated based on these modified samples, with the resulting differences in acceptance taken as a systematic uncertainty depending on the resonance mass. Additionally, the induced changes on the shape of the reconstructed resonances (independently of the yield) are propagated as uncertainties on the signal line-shape; these are taken to be 2% (11%) on the jet mass scale (resolution) as evaluated in [48] and are based on differences in the jet mass by selecting boosted hadronically decaying W bosons and comparing the reconstructed jet mass peak and resolution in the data and MC. In addition, we consider the effect of the efficiency of the selection requirement on τ_{21} on the signal acceptance. Based on previous studies [48], it is known that there are disagreements in the efficiency of the two-prong tagger in data and in MC. In [48], the efficiency of the two-prong tagger for W bosons was measured in $t\bar{t}$ events in both data and MC using the same pileup method and τ_{21} selection as we apply in this analysis. Differences in the resulting tagging efficiencies are driven by the discrepancy between data and MC in the τ_{21} distribution. The ratio of the efficiency in data and simulation yields a two-prong tagging scale factor and is measured to be 0.94 ± 0.08 for $\tau_{21} < 0.45$. Since we tag two two-prong jets (i.e. both jets are required to pass the τ_{21} selection), we apply this scale factor squared to the signal yield, giving total scale factor of 0.88 ± 0.15. The uncertainty on this scale factor is taken as a systematic uncertainty on the signal acceptance. Finally, we also consider additional systematic uncertainties on the signal acceptance which originate from the following sources: integrated luminosity (2.7%) [15]; trigger (2%); parton distribution functions (12%) [49]; and pileup (1.5%). In addition, we consider statistical uncertainties arising from the limited number of MC events generated.

The systematic uncertainties on the background estimates are summarized in Table 4. For the non-resonant QCD multijets background estimate using the ABCD method, we consider three possible sources of uncertainties. First, we assign a systematic uncertainty based on the closure test described in Section 6 found to be 10% and is applied to the overall yield of the background prediction. In addition, we apply an uncertainty on the transfer factor shape from the fit parameter errors and the statistical uncertainties on the number of events in region C; these uncertainties are applied bin-by-bin as a systematic affecting the shape of the average pruned jet mass distribution for the QCD mutijets background estimate. We also assign systematic uncertainties to the $t\bar{t}$ and other resonant background estimates. From the data/MC scale factor study performed using the $t\bar{t}$ control sample described in Section 6 we include a 50% systematic uncertainty on the overall modeling of the SM MC samples used. Finally, the statistical uncertainties of the MC samples are also considered bin-by-bin.

8 Results

Figure 2 shows the average pruned jet mass distribution after the final event selection is applied for data as well as the total background prediction described in Section 6; the overall uncertainty on the background predictions described in Section 7 is also shown. We do not observe an excess of events in data over the background prediction, and therefore we proceed to set 95 % confidence level (CL) upper limits on the pair production cross section of stops via the RPV coupling λ''_{312}. We assume a 100% branching ratio of the RPV λ''_{312} stops into two light quarks.

These exclusion limits are computed using the modified frequentist approach for confidence

Table 3: Overview of the systematic uncertainties on the signal acceptance by source.

Source of Systematic	Effect	Value
Luminosity	Yield	2.7%
Trigger	Yield	2%
Pileup	Yield	1.5%
PDF	Yield	12%
Two-prong Tagger Scale Factor	Yield	17%
Jet Energy Scale	Yield	0.8%-5%
Jet Energy Resolution	Yield	0.6%-3%
MC Statistics	-	bin-by-bin
Jet Mass Scale	Resonance Shape	2%
Jet Mass Resolution	Resonance Shape	11%

Table 4: Overview of the systematic uncertainties on the background prediction by source.

Background	Source of Systematic	Effect	Value
QCD ABCD method:	Closure	Yield	10%
	Transfer Factor Fit Uncertainty	Shape	0.8%-8%
	Statistics in Sideband Region (C)	Shape	bin-by-bin
Resonant backgrounds:	Systematic in MC Backgrounds	Yield	50%
	MC Statistics	Shape	bin-by-bin

levels (CLs), using the binned profile likelihood as the test statistic in the asymptotic approximation [50, 51]. Results are obtained from combined signal and background binned likelihood fits to the average pruned jet mass in data. For each stop mass scenario, only bins of average pruned jet mass (of width 5 GeV) within 2 σ of a Gaussian peak centered at the generated mass are included in the likelihood and combined. For each bin used in the likelihood the individual background components and signal are allowed to float within statistical errors with no correlations between bins; systematic uncertainties affecting the yield as indicated in Tables 3 and 4 are assumed to be correlated between bins, whereas the rest are treated as uncorrelated. Systematic uncertainties described in Section 7 are treated as nuisance parameters, which are profiled, and modeled with log-normal priors, except for the uncertainty on the number of events in the sideband region (C) which is modeled with a Gamma prior.

Fig. 3 shows the observed and expected 95% CL upper limits on the stop pair production cross section as a function of stop mass. The dashed pink line indicates the NLO + NLL theoretical predictions for stop production. The increase in the limit for higher masses around 300 GeV is due to the drop in the fraction of signal events accepted by the selection criteria due to the decrease in events produced with the boosted topology, as mentioned in Section 3. The production of stops undergoing RPV decays with the λ''_{312} coupling is excluded at 95% CL for stop masses in the range from 80 to 240 GeV.

9 Summary

A search has been performed for pair production of boosted resonances decaying to quarks giving a dijet signature from proton-proton collisions from the LHC at $\sqrt{s} = 13$ TeV with the CMS detector. The distribution in the average pruned jet mass of selected events has been used to search for an excess compatible with a resonance signal above the SM background

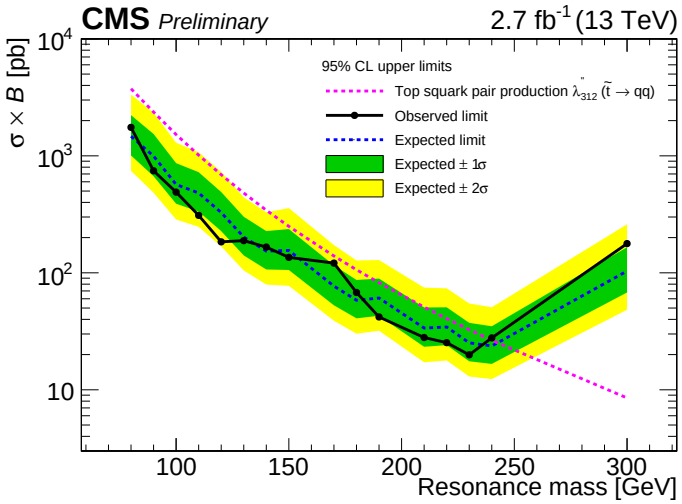

Figure 3: Observed and expected 95% CL upper limits on cross section vs. stop mass. The dashed pink line shows the NLO + NLL theoretical predictions for stop pair production.

estimate. No significant deviation is found. Exclusion limits are set on the top squark pair production cross section with decays through the RPV SUSY coupling λ''_{312} to light-flavor jets at 95% confidence level. We exclude stop masses between 80 GeV and 240 GeV.

References

[1] H. P. Nilles, "Supersymmetry, supergravity and particle physics", *Phys. Rep.* **110** (1984) 1, doi:10.1016/0370-1573(84)90008-5.

[2] H. E. Haber and G. L. Kane, "The search for supersymmetry: Probing physics beyond the standard model", *Phys. Rep.* **117** (1985) 75, doi:10.1016/0370-1573(85)90051-1.

[3] M. Papucci, J. Ruderman, and A. Weiler, "Natural SUSY endures", *JHEP* **09** (2012) 035, doi:10.1007/JHEP09(2012)035.

[4] R. Barbieri and G. F. Giudice, "Upper bounds on supersymmetric particle masses", *Nucl. Phys. B* **306** (1988) 63, doi:10.1016/0550-3213(88)90171-X.

[5] S. Dimopoulos and G. F. Giudice, "Naturalness constraints in supersymmetric theories with nonuniversal soft terms", *Phys. Lett. B* **57** (1995) 573, doi:10.1016/0370-2693(95)00961-J, arXiv:hep-ph/9507282.

[6] R. Barbieri and D. Pappadopulo, "S-particles at their naturalness limits", *JHEP* **10** (2009) 61, doi:10.1088/1126-6708/2009/10/061, arXiv:0906.4546.

[7] A. G. Cohen, D. B. Kaplan, and A. E. Nelson, "The more minimal supersymmetric standard model", *Phys. Lett. B* **388** (1996) 588, doi:10.1016/S0370-2693(96)01183-5, arXiv:hep-ph/9607394.

[8] R. Barbier et al., "R-Parity-violating supersymmetry", *Phys. Rep.* **420** (2005) 1, doi:10.1016/j.physrep.2005.08.006.

[9] J. A. Evans and Y. Kats, "LHC Coverage of RPV MSSM with Light Stops", *JHEP* **1304** (2013) 28, doi:10.1007/JHEP04(2013)028, arXiv:1209.0764.

[10] CDF Collaboration, "Search for Pair Production of Strongly Interacting Particles Decaying to Pairs of Jets in $p\bar{p}$ Collisions at $\sqrt{s} = 1.96$TeV", *Phys. Rev. Lett.* **111** (2013), no. 3, 031802, doi:10.1103/PhysRevLett.111.031802, arXiv:1303.2699.

[11] CMS Collaboration, "Search for pair-produced resonances decaying to jet pairs in protonproton collisions at $\sqrt{s}$=8 TeV", *Phys. Lett.* **B747** (2015) 98–119, doi:10.1016/j.physletb.2015.04.045, arXiv:1412.7706.

[12] ATLAS Collaboration, "A search for pair produced resonances in four jets final states in proton-proton collisions at $\sqrt{s}$=13 TeV with the ATLAS experiment", Technical Report ATLAS-CONF-2016-084, CERN, Geneva, Aug, 2016.

[13] ATLAS Collaboration, "A search for **R**-parity violating scalar top decays in all-hadronic final states with the ATLAS detector in $\sqrt{\mathbf{s}} = \mathbf{8}$ TeV **pp** collisions", Technical Report ATLAS-CONF-2015-026, CERN, Geneva, 2015.

[14] ATLAS Collaboration, "A search for R-parity violating decays of the top squark in four jet final states with the ATLAS detector at $\sqrt{s} = 13$ TeV", Technical Report ATLAS-CONF-2016-022, CERN, Geneva, May, 2016.

[15] CMS Collaboration, "CMS Luminosity Measurement for the 2015 Data Taking Period", Technical Report CMS-PAS-LUM-15-001, CERN, Geneva, 2016.

[16] CMS Collaboration, "The CMS experiment at the CERN LHC", *JINST* **3** (2008) S08004, doi:10.1088/1748-0221/3/08/S08004.

[17] M. Dasgupta, A. Fregoso, S. Marzani, and G. P. Salam, "Towards an understanding of jet substructure", *JHEP* **09** (2013) 029, doi:10.1007/JHEP09(2013)029, arXiv:1307.0007.

[18] D. Adams et al., "Towards an Understanding of the Correlations in Jet Substructure", *Eur. Phys. J.* **C75** (2015), no. 9, 409, doi:10.1140/epjc/s10052-015-3587-2, arXiv:1504.00679.

[19] CMS Collaboration, "Pileup Removal Algorithms", Technical Report CMS-PAS-JME-14-001, CERN, Geneva, 2014.

[20] J. Alwall et al., "The automated computation of tree-level and next-to-leading order differential cross sections, and their matching to parton shower simulations", *JHEP* **07** (2014) 079, doi:10.1007/JHEP07(2014)079, arXiv:1405.0301.

[21] T. Sjostrand, S. Mrenna, and P. Z. Skands, "A Brief Introduction to PYTHIA 8.1", *Comput. Phys. Commun.* **178** (2008) 852–867, doi:10.1016/j.cpc.2008.01.036, arXiv:0710.3820.

[22] E. Farhi and L. Susskind, "Grand Unified Theory with Heavy Color", *Phys. Rev. D* **20** (1979) 3404, doi:10.1103/PhysRevD.20.3404.

[23] W. J. Marciano, "Exotic New Quarks and Dynamical Symmetry Breaking", *Phys. Rev. D* **21** (1980) 2425, doi:10.1103/PhysRevD.21.2425.

[24] P. H. Frampton and S. L. Glashow, "Unifiable Chiral Color with Natural Glashow-Iliopoulos-Maiani Mechanism", *Phys. Rev. Lett.* **58** (1987) 2168, doi:10.1103/PhysRevLett.58.2168.

[25] P. H. Frampton and S. L. Glashow, "Chiral Color: An Alternative to the Standard Model", *Phys. Lett. B* **190** (1987) 157, doi:10.1016/0370-2693(87)90859-8.

[26] R. S. Chivukula, M. Golden, and E. H. Simmons, "Multi-jet Physics at Hadron Colliders", *Nucl. Phys. B* **363** (1991) 83, doi:10.1016/0550-3213(91)90235-P.

[27] C. Borschensky et al., "Squark and gluino production cross sections in pp collisions at $\sqrt{s}$ = 13, 14, 33 and 100 TeV", *Eur. Phys. J.* **C74** (2014), no. 12, 3174, doi:10.1140/epjc/s10052-014-3174-y, arXiv:1407.5066.

[28] W. Beenakker, R. Höpker, M. Spira, and P. M. Zerwas, "Squark and gluino production at hadron colliders", *Nucl. Phys. B* **492** (1997) 51, doi:10.1016/S0550-3213(97)80027-2, arXiv:hep-ph/9610490.

[29] A. Kulesza and L. Motyka, "Threshold Resummation for Squark-Antisquark and Gluino-Pair Production at the LHC", *Phys. Rev. Lett.* **102** (2009) 111802, doi:10.1103/PhysRevLett.102.111802, arXiv:0807.2405.

[30] A. Kulesza and L. Motyka, "Soft gluon resummation for the production of gluino-gluino and squark-antisquark pairs at the LHC", *Phys. Rev. D* **80** (2009) 095004, doi:10.1103/PhysRevD.80.095004, arXiv:0905.4749.

[31] W. Beenakker et al., "Soft-gluon resummation for squark and gluino hadroproduction", *JHEP* **12** (2009) 041, doi:10.1088/1126-6708/2009/12/041, arXiv:0909.4418.

[32] W. Beenakker et al., "Squark and gluino hadroproduction", *Int. J. Mod. Phys. A* **26** (2011) 2637, doi:10.1142/S0217751X11053560, arXiv:1105.1110.

[33] W. Beenakker et al., "NLO+NLL squark and gluino production cross-sections with threshold-improved parton distributions", *Eur. Phys. J.* **C76** (2016), no. 2, 53, doi:10.1140/epjc/s10052-016-3892-4, arXiv:1510.00375.

[34] P. Skands, S. Carrazza, and J. Rojo, "Tuning PYTHIA 8.1: the Monash 2013 Tune", *Eur. Phys. J. C* **74** (Apr, 2014) 3024. 57 p. Comments: 57 pages.

[35] P. Nason, "A New Method for Combining NLO QCD with Shower Monte Carlo Algorithms", *J. High Energy Phys.* **11** (Sep, 2004) 040. 29 p.

[36] S. Frixione, P. Nason, and C. Oleari, "Matching NLO QCD computations with Parton Shower simulations: the POWHEG method", *J. High Energy Phys.* **11** (Sep, 2007) 070. 91 p. Comments: 91 pages, 2 figures.

[37] S. Alioli, P. Nason, C. Oleari, and E. Re, "A general framework for implementing NLO calculations in shower Monte Carlo programs: the POWHEG BOX", Technical Report arXiv:1002.2581, Feb, 2010. Comments: 57 pages, 4 figures.

[38] GEANT4 Collaboration, "Geant4—a simulation toolkit", *Nucl. Instrum. Meth. A* **506** (2003) 250, doi:10.1016/S0168-9002(03)01368-8.

[39] CMS Collaboration, "Commissioning of the Particle-flow Event Reconstruction with the first LHC collisions recorded in the CMS detector", CMS Physics Analysis Summary CMS-PAS-PFT-10-001, 2010.

[40] M. Cacciari, G. P. Salam, and G. Soyez, "The Anti-k_t Jet Clustering Algorithm", *JHEP* **04** (2008) 63, doi:10.1088/1126-6708/2008/04/063, arXiv:0802.1189.

[41] M. Cacciari, G. P. Salam, and G. Soyez, "FastJet User Manual", *Eur. Phys. J.* **C72** (2012) 1896, doi:10.1140/epjc/s10052-012-1896-2, arXiv:1111.6097.

[42] D. Krohn, J. Thaler, and L.-T. Wang, "Jet Trimming", *JHEP* **02** (2010) 084, doi:10.1007/JHEP02(2010)084, arXiv:0912.1342.

[43] CMS Collaboration, "Determination of jet energy calibration and transverse momentum resolution in CMS", *JINST* **6** (2011) 11002, doi:10.1088/1748-0221/6/11/P11002, arXiv:1107.4277.

[44] CMS Collaboration, "Jet Performance in pp Collisions at 7 TeV", CMS Physics Analysis Summary CMS-PAS-JME-10-003, 2010.

[45] S. D. Ellis, C. K. Vermilion, and J. R. Walsh, "Recombination Algorithms and Jet Substructure: Pruning as a Tool for Heavy Particle Searches", *Phys. Rev.* **D81** (2010) 094023, doi:10.1103/PhysRevD.81.094023, arXiv:0912.0033.

[46] J. Thaler and K. Van Tilburg, "Maximizing Boosted Top Identification by Minimizing N-subjettiness", *JHEP* **02** (2012) 093, doi:10.1007/JHEP02(2012)093, arXiv:1108.2701.

[47] CMS Collaboration, "Identification of b quark jets at the CMS Experiment in the LHC Run 2", Technical Report CMS-PAS-BTV-15-001, CERN, Geneva, 2016.

[48] CMS Collaboration, "Search for massive resonances decaying into pairs of boosted W and Z bosons at $\sqrt{s}$ = 13 TeV", Technical Report CMS-PAS-EXO-15-002, CERN, Geneva, 2015.

[49] NNPDF Collaboration, "Parton distributions for the LHC Run II", *JHEP* **04** (2015) 040, doi:10.1007/JHEP04(2015)040, arXiv:1410.8849.

[50] A. L. Read, "Presentation of search results: the CL s technique", *Journal of Physics G: Nuclear and Particle Physics* **28** (2002), no. 10, 2693.

[51] T. Junk, "Confidence level computation for combining searches with small statistics", *Nuclear Instruments and Methods in Physics Research Section A: Accelerators, Spectrometers, Detectors and Associated Equipment* **434** (1999), no. 2, 435 – 443, doi:http://dx.doi.org/10.1016/S0168-9002(99)00498-2.